International Journal of Nanomedicine

Dovepress
open access to scientific and medical research

Open Access Full Text Article

ORIGINAL RESEARCH

Synthesis and characterization of low-toxicity N-caprinoyl-N-trimethyl chitosan as self-assembled micelles carriers for osthole

This article was published in the following Dove Press journal:
International Journal of Nanomedicine
25 September 2013
Number of times this article has been viewed

Xiao-juan Hu[1,*]
Yang Liu[1,*]
Xiao-feng Zhou[2,3]
Qiao-ling Zhu[1]
Yong-yan Bei[1]
Ben-gang You[1]
Chun-ge Zhang[1]
Wei-liang Chen[1]
Zhou-li Wang[1]
Ai-jun Zhu[1]
Xue-nong Zhang[1]
Yu-jiang Fan[4]

[1]Department of Pharmaceutics, College of Pharmaceutical Sciences, Soochow University, Suzhou, People's Republic of China; [2]College of Radiological Medicine and Protection, Soochow University, People's Republic of China; [3]Changshu Hospital of Traditional Chinese Medicine, Changshu, People's Republic of China; [4]Department of Clinical Laboratory, Second People's Hospital of Akesu, Akesu, People's Republic of China

*These authors contributed equally to this work

Abstract: Novel amphiphilic chitosan derivatives (N-caprinoyl-N-trimethyl chitosan [CA-TMC]) were synthesized by grafting the hydrophobic moiety caprinoyl (CA) and hydrophilic moiety trimethyl chitosan to prepare carriers with good compatibility for poorly soluble drugs. Based on self-assembly, CA-TMC can form micelles with sizes ranging from 136 nm to 212 nm. The critical aggregation concentration increased from 0.6 mg · L^{-1} to 88 mg · L^{-1} with decrease in the degree of CA substitution. Osthole (OST) could be easily encapsulated into the CA-TMC micelles. The highest entrapment efficiency and drug loading of OST-loaded CA-TMC micelles(OST/CA-TMC) were 79.1% and 19.1%, respectively. The antitumor efficacy results show that OST/CA-TMC micelles have significant antitumor activity on Hela and MCF-7 cells, with a 50% of cell growth inhibition (IC50) of 35.8 and 46.7 μg · mL^{-1}, respectively. Cell apoptosis was the main effect on cell death of Hela and MCF-7 cells after OST administration. The blank micelles did not affect apoptosis or cell death of Hela and MCF-7 cells. The fluorescence imaging results indicated that OST/CA-TMC micelles could be easily uptaken by Hela and MCF-7 cells and could localize in the cell nuclei. These findings suggest that CA-TMC micelles are promising carriers for OST delivery in cancer therapy.

Keywords: N-trimethyl chitosan, micelle solubilization, antitumor activity

Introduction

Osthole (OST) (7-methoxy-8-[3-methylpent-2-enyl] coumarin) is an active coumarin constituent isolated from the dried fruit of *Cnidium monnieri (L) Cusson*, a well-known traditional Chinese medicine with various pharmacological and biological applications; OST has been used for its antidiabetic, antiosteoporotic, anti-inflammatory, neuroprotective, and estrogen-like effects.[1–5] Accumulating evidence indicates that OST exerts an antitumor effect by inhibiting tumor cell growth and inducing apoptosis.[6–9] OST has synergistic effects with other drugs and exhibits decreased side effects.[10,11] However, OST showed insolubility in water, subabsorption through oral administration, and the bioavailability was limited in application.[12]

Chitosan, a naturally cationic polysaccharide composed of glucosamine and N-acetyl-glucosamine, has many interesting properties that are useful in biological applications, including biodegradable nontoxicity, high biocompatibility, and antimicrobial activity.[13–15] But chitosan has poor aqueous solubility at physiological pH, which is disadvantageous for our research. N-trimethyl chitosan (TMC) is a partially quaternized derivative of chitosan first synthesized by Muzzarelli and Tanfani[16] in an attempt to increase the solubility of chitosan in water at neutral and basic pH values. The increase in solubility is achieved by replacing the primary amino group on the

Correspondence: Xue-nong Zhang
The Department of Pharmaceutics, College of Pharmaceutical Science, Soochow University, DuShuHu High Education Zone, Su Zhou, Jiang Su Province, 215123, People's Republic of China
Tel +86 0512 65 88 2087
Fax +86 0512 65 88 2087
Email zhangxuenong@163.com

Yu-jiang Fan
The Clinical Laboratory of the Second People's Hospital of Akesu, Cultural Road No 32, Akesu 843000, Xinjiang Province, People's Republic of China
Tel +86 0997 25 9 3055
Fax +86 0997 25 9 3055
Email 13899251802@163.com

C-2 position of chitosan with quaternary amino groups.[17] It has been shown that TMC can decrease the transepithelial electrical resistance (TEER) of Caco-2 cell monolayers and increase the transport of peptide and protein drugs both in vitro and in vivo.[18,19] Up to date, TMC has received considerable attention in drug and gene delivery, not only for use by peroral route[20] but also by ocular,[21] intranasal,[22] pulmonary,[23] and rectal[24] routes. The drug loading (DL) of TMC for OST was very low, so the solubilization of OST was limited in previous studies.

Recently, polymeric micelles have attracted increasing attention as promising vehicles for poorly soluble drugs.[25,26] Polymeric micelles are self-assemblies of amphiphilic block copolymers in aqueous media. The high potential of polymeric micelles as drug carriers lies in their unique characteristics, such as nanoscale size, thermodynamic stability, and unique core−shell architecture.[27] Hydrophobic drugs can be solubilized into the hydrophobic core structures of polymer micelles. The hydrophilic shell surrounding the micellar core can prevent intermicellar aggregation or precipitation, protein adsorption, and cell adhesion from happening.[28,29] It has been reported that highly tumor-specific delivery of anticancer agents was achieved using polymeric micelles as carriers.[30,31]

To overcome the insolubility and subabsorption problem of OST, we designed an amphiphilically modified chitosan derivative, N-caprinoyl -N-trimethyl chitosan and tested the potential of CA-TMC as a micellar carrier for OST. This was the first time that hydrophobic moiety caprinoyl chains were conjugated to the chitosan backbone of TMC to obtain novel amphiphilic chitosan derivatives; the positive charge of TMC was the hydrophilic shell surrounding the micellar core to enhance the absorption of the OST. Since the self-assembling abilities and biocompatibilities of the novel chitosan amphiphilic derivatives were important for their use as micellar carriers, the critical micelle concentration, biocompatibilities, effect of degree of quaternization (DQ) of CA-TMC, degree of substitution (DS) of caprinoyl chains of CA-TMC on the drug-loading capacity, stability, and other properties were investigated in detail. Finally, the effect of OST and OST-loaded micelles were compared to test targets in this study.

Materials and methods

Materials and animals

Chitosan with a deacetylation degree of 93.1% and a molecular weight (MW) of 8 kDa to 10 kDa was supplied by Xincheng Biological Industrial Co, Ltd (Nantong, People's Republic of China). OST with 98% purity was provided by Langze Pharmaceutical Science and Technology Co, Ltd (Nanjing, People's Republic of China). Iodomethane (CH_3I), 1-methyl-2-pyrrolidinone (NMP), ethanol (EtOH), diethyl ether (Et2O), dichloromethane (CH_2Cl_2), sodium chloride (NaCl), and sodium hydroxide (NaOH) were obtained from Sinopharm Chemical Reagent Co, Ltd (Shanghai, People's Republic of China). Sodium iodide (NaI), 1-(3-dimethylaminopropyl)-3-ethylcarbodiimide hydrochloride (EDC·HCl), and N-hydroxysuccinimide (NHS) were purchased from Aladdin Reagents (Shanghai, People's Republic of China). Capric acid, palmitic acid, 3-(4,5-dimethyl-2-thiazo-lyl)-2,5-diphenyl-2H-tetrazolium bromide (MTT), and dimethyl sulfoxide (DMSO) were purchased from Sigma-Aldrich (St Louis, MO, USA). Newborn bovine serum and Roswell Park Memorial Institute medium (RPMI) 1640 medium were provided by Solarbio Bioscience and Technology Co, Ltd (Shanghai, People's Republic of China). All other chemicals were of analytical grade and used without further purification.

Human cervical cancer cells (Hela), breast cancer cells (MCF-7), and human liver cells (HL7702) were provided by the pharmacology laboratory of Soochow University (Suzhou, People's Republic of China). Kunming mice (60, half male, 18 to 22 g) and three rabbits (male, 2.3 kg) were obtained from the Experimental Animal Center of Soochow University. All animals were pathogen-free and had free access to food and water. All animal experiments were carried out in compliance with the Experimental Animal Center, Soochow University.

Synthesis of CA-TMC

Synthesis of TMC

TMC was synthesized by reductive methylation of chitosan through a chemical reaction between chitosan and CH_3I, in the presence of NaOH, based on the methods described by Snyman et al.[32]

Synthesis of TMC1

Chitosan (2 g) and CH_3I (4.8 g) were dissolved in 80 mL of NMP on a water bath at 60°C, with stirring. After the chitosan was dissolved, 11 mL of 15% NaOH solution was added, followed by 11.5 mL of CH_3I, both with stirring. The mixture was stirred for 1 hour. The product was precipitated using EtOH and subsequently isolated by centrifugation. The substratum solid (1) was collected, and then, the precipitate was dissolved in 15% (w/v) of NaCl to replace the iodide ions with chloride ions. The suspension was subsequently dialyzed (10KaD,

regenerated cellulose, Spectrum Laboratories, Inc., USA) with deionized water for 3 days to remove inorganic materials. The suspension was then freeze-dried by an ALPHA1-4/LSC lyophilizer (Martin Christ GmbH, Osterode, Germany) to produce cotton-like TMC chloride powder.

Synthesis of TMC2

The N-trimethyl chitosan iodide (1) was dissolved in 80 mL of NMP and heated to 60°C, thus removing most of the absorbed ether. Subsequently, 4.8 g of NaI, 11 mL of 15% NaOH solution, and 11.5 mL of CH_3I were added, with rapid stirring. Then, the mixture was heated on a water bath at 60°C for 45 minutes. The product was precipitated using EtOH and subsequently isolated by centrifugation. The substratum solid (2) was collected. Then, the products were treated using the same process as that in TMC1.

Synthesis of TMC3

The N-trimethyl chitosan iodide (2) was dissolved in 80 mL of NMP and heated to 60°C, thus removing most of the absorbed ether. Subsequently, 4.8 g of NaI, 11 mL of 15% NaOH solution, and 11.5 mL of CH_3I were added with rapid stirring, and then, the mixture was heated on a water bath at 60°C for 1 hour. The products were treated using the same process as that in TMC1.

Synthesis of CA-TMC

Capric acid (0.172 g) was dissolved in 20 mL of dry CH_2Cl_2 on a water bath at 40°C, with stirring. After the capric acid was dissolved, 0.384 g of EDC·HCl was added. After the EDC·HCl was dissolved, 0.115 g of NHS was added with stirring. The mixture was stirred for 2 hours. CH_2Cl_2 was then removed by rotary evaporation. The product was redissolved in 50 mL of CH_3OH with stirring, on a water bath at 70°C. Then, the product was dissolved in CH_3OH, with 20 mL of the TMC water solution (about 1.0 mmol free amino groups) being slowly dropped into the mixture. The mixture was stirred for 24 hours. After the reaction, the product was passed through a filter with MW of 10,000 (regenerated cellulose, Spectrum Laboratories, Inc.) for 2 days to filter in 30% EtOH solution. Then, the product was filtered in deionized water for another 3 days. After 5 days of filtration, the polymer was dried in an AIPHA1-4/LSC lyophilizer.

Structural characterization of CA-TMC

Fourier transform infrared (FTIR) spectra of the derivatives were measured in the 4,000 to 400 cm^{-1} region using a Prostar LC240 FTIR spectrometer (Varian Inc, Palo Alto, CA, USA) in potassium bromide (KBr) discs.

Proton nuclear magnetic resonance (^{1}H-NMR) spectra of chitosan and chitosan derivatives were recorded on a Unity Inova 400 MHz spectrometer (Varian Inc) using CF3COOD/D_2O and DMSO-d6 as solvents, at 25°C.

Elemental analysis (C, N) was performed on a Vario EL-III elemental analyzer (Elementar Analysensysteme GmbH, Hanau, Germany). The percentages of carbon, nitrogen, and sulfur were estimated. The DQ of trimethyl and the DS of caprinoyl were calculated based on the following formulas:[33]

$$DQ\% = \frac{C/N(mol)_{TMC} - C/N(mol)_{chitosan}}{3} \times 100\% \quad (1)$$

$$DS\% = \frac{C/N(mol)_{CA\text{-}TMC} - C/N(mol)_{TMC}}{10} \times 100\%. \quad (2)$$

Measurement of critical micelle concentration (CMC)

The CMC of CA-TMC was measured by pyrene (>98%; Sigma-Aldrich), which acted as a hydrophobic probe in fluorescence spectroscopy (LS55 Fluorescence Spectrometer; PerkinElmer, Waltham, MA, USA).[34,35] A specific amount of pyrene in acetone was added to a series of 10 mL vials, and then acetone was evaporated at room temperature. A certain amount of various concentrations of CA-TMC solutions (2×10^{-6} mg·mL^{-1} to 1.0 mg·mL^{-1}) was added to the vials (the final concentration of pyrene was controlled at 6.0×10^{-7} mol·mL^{-1}) and sonicated for 30 minutes at 28°C. The sample solutions were heated at 40°C for 3 hours to equilibrate the pyrene and the micelles, and then left to cool overnight at room temperature. Fluorescence excitation spectra were measured at the excitation wavelength (λex) of 335 nm. Both excitation and emission bandwidths were set at 2.5 nm, and the spectra were accumulated with an integration time of 240 nm·min^{-1}. The emission wavelength for the emission spectra was 350 nm to 450 nm.

Biocompatibility evaluation

Cytocompatibility

The cells were maintained in RPMI-1640 medium supplemented with 10% (v/v) heat-inactivated (56°C, 30 minutes) fetal bovine serum and 100 U·mL^{-1} penicillin G-streptomycin (Beyotime Institute of Biotechnology, Haimen, People's Republic of China) at 37°C in a humidified incubator (5% CO_2). Cells at the logarithmic growth phase were seeded at a density of 3×10^4 cells·mL^{-1} in

96-well culture plates, with a total volume of 200 μL per well. Cells were incubated for 24 hours at 37°C and 5% CO_2 to allow culture cell adhesion. Then, the culture medium was aspirated and replaced with fresh medium supplemented with corresponding concentrations of CA-TMC. Following incubation for 2 days, 20 μL of MTT solution (5 $mg \cdot mL^{-1}$ dissolved in pH7.4 phosphate-buffered saline [PBS] solution) was added to each well. The plate continued to incubate for 4 hours, and 150 μL of DMSO was introduced to dissolve the insoluble blue formazan precipitate produced by MTT reduction. The plate was shaken for 3 minutes, and the absorbance (A) was measured at 492 nm with an enzyme immunoassay instrument (Bio-tek ELX800 enzyme immunoassay instrument, Bio Tek Instruments, Inc, Winooski, VT, USA). The cytotoxicity of CA-TMC was expressed and calculated using the following formula:

$$CV\% = \frac{A_1 - A_0}{A_2} \times 100\%, \quad (3)$$

where A_0, A_1, and A_2 were the average A of the medium, treated group, and control group, respectively.

Hemolysis test

The hemolysis by CA-TMCs was determined using low-molecular-weight surfactants (including Tween 80 and F188) as controls. Initially, 2 mL of CA-TMC micelles, Tween 80 and F188 solution were placed in test tubes at 37°C for further usage. Subsequently, 20 mL of fresh blood from three rabbits were depleted of fibrinogen and centrifuged at 2500 $r \cdot min^{-1}$ for 10 minutes. The erythrocyte pellets were washed with saline and then, resuspended in saline to achieve 2% (v/v) erythrocyte dispersion.

The hemolysis test was performed by the following method: the red blood cell (RBC) suspension (2 mL) was added to 2 mL of samples until the ultimate concentrations of CA-TMC micelles, Tween 80, and F188 ranged from 0.1 to 2 $mg \cdot mL^{-1}$. After incubating at 37°C for 2 hours, the above suspension was centrifuged at 2,500 $r \cdot min^{-1}$ for 10 minutes to remove intact RBC. The supernatant was collected and analyzed for released hemoglobin with a UV-2600 Spectrophotometer (Shimadzu Corporation, Kyoto, Japan) at 416 nm (n = 3). To obtain 0 and 100% hemolysis, 2 mL of saline and 2 mL of distilled water was added to 2 mL of RBC suspension, respectively. The degree of hemolysis of F188 and Tween 80 were calculated with the following equation 4. The degree of hemolysis by CA-TMC was calculated using equation 5.

$$\text{Hemolysis } (\%) = \frac{A_{sample} - A_{0\%}}{A_{100\%} - A_{0\%}} \times 100\%, \quad (4)$$

$$\text{Hemolysis } (\%) = \frac{A_{sample} - A_{sample(saline)\%}}{A_{100\%} - A_{0\%}} \times 100\%, \quad (5)$$

where A_{sample}, A_{100}, and A_0 were the absorbance of samples, a solution of 100% hemolysis, and a solution of 0% hemolysis. The turbidity of samples was compensated for by using a sample solution without erythrocytes as a blank control.

Acute toxicity

Kunming mice (18 g to 22 g) were randomly divided into six groups (n = 8, 50% male, 50% female). The mice received a single injection of CA-TMC micellar solution at doses of 261.0, 307.1, 361.3, 425.0, and 500.0 $mg \cdot kg^{-1}$, through the tail vein. An injection of 0.9% physiological saline was administered as control, through the tail vein. The mice were observed for 2 weeks in all groups, and the number of surviving mice was recorded. The median lethal dose (LD50) and 95% confidence limits were calculated using the Bliss method.[34] The histopathological effects of blank CA-TMC micelles on various organs, such as the heart, liver, spleen, lung, and kidney, were investigated after intravenous (IV) administration of micellar solution at a half-dose level of LD50.[34] The histopathological changes in each organ were observed under an Olympus BX-40 light microscope (Olympus Corporation, Tokyo, Japan) at day 8 after the treatment.

OST-loaded CA-TMC micelles

Preparation and characterization of OST-loaded CA-TMC micelles

OST was loaded into the micelles by the addition of 300 μL of OST solution (20 $mg \cdot mL^{-1}$) in EtOH to 20 mL of copolymer solution of CA-TMC (1 $mg \cdot mL^{-1}$) in water. The mixture solution was made using a JY92-II ultrasonic cell smash device (Ningbo Scientz Bio-Technology Co, Ltd, Ningbo City, People's Republic of China) at 200 W for 5 minutes, in an ice bath. The excess drug was removed by filtration through 0.45 μm PVDF filters (Lubitech Technologies Ltd, Shanghai, People's Republic of China). The particle size and zeta-potential of the micelles were respectively determined by dynamic light scattering (DLS) (Nicomp-380ZLS; Particle Sizing Systems Inc, Port Richey, FL, USA) combined with transmission electron microscopy (Bruker Dimension Icon atom force microscopy) (TEM) (Tecnai™ G220; FEI Co, Hillsboro, OR, USA) and atomic force microscopy (AFM) (Bruker, Billerica, MA, USA) to observe the form of OST-loaded micelles. Measurements were performed in triplicate,

in demineralized water. The encapsulation efficiency (EE) and DL of OST were determined by high-performance liquid chromatography (HPLC) (Agilent 1100 series, Agilent Technologies, Santa Clara, CA, USA). A total of 1 mg of OST/CA-TMC freeze-dried powder was added into 10 mL of methanol, subjected to an ultrasonic meter at 300 W for 5 minutes, in an ice bath, and then centrifuged at 10,000 $r \cdot min^{-1}$ for 10 minutes. The supernatant was reserved for detection. The mobile phase consisted of acetonitrile/water (60:40 v/v). The phase column was an ODS-2 Hypersil C18 (4.6 × 250 mm, 5 μm; Thermo Fisher Scientific, Waltham, MA, USA). The column temperature was maintained at 25°C. The flow rate was set at 1.0 $mL \cdot min^{-1}$. The detection wavelength was 322 nm. A sample of 20 μL of supernatant was injected. The HPLC was calibrated with standard solutions of 0.5 $\mu g \cdot mL^{-1}$ to 100 $\mu g \cdot mL^{-1}$ OST dissolved in methanol (correlation coefficient of $R^2 = 0.9965$). The EE% and DL% values were calculated as follows:

$$EE\% = \frac{W_T}{W_U} \times 100\%, \quad (6)$$

$$DL\% = \frac{W_T}{W_M} \times 100\%, \quad (7)$$

where W_T is the weight of OST detected, W_U is the weight of OST used, and W_M is the weight of all the OST-loaded micelles.

In vitro drug release studies of OST-loaded micelles

OST-loaded micelles (5 mL, 1 $mg \cdot mL^{-1}$) in dialysis bags (Beijing Solaarbio Science & Technology Co.,Ltd., Beijing, People's Republic of China) (cutoff MW: 3,500) were placed in 100 mL of PBS (0.1 $mol \cdot L^{-1}$, pH 5.0 and 7.4, and containing 10% EtOH). OST was subjected to the same conditions. The systems were then immersed in a thermostatic bath with a speed of 100 $r \cdot min^{-1}$, at 37°C. At appropriate intervals, 2 mL of the solution samples were withdrawn from the vials and replaced by 2 mL of fresh PBS. The samples were centrifuged at 10,000 $r \cdot min^{-1}$ for 30 minutes. Then, 20 μL of the supernatant was assayed by HPLC.

In vitro antitumor activity of OST-loaded micelles

MTT assay

The proliferation of Hela and MCF-7 cells following treatment with OST and OST/CA-TMC2 micelles was measured using MTT. Hela and MCF-7 cells (1×10^4) were seeded in 96-well plates and allowed to adhere overnight, and then were separately treated with various concentrations of OST and OST/CA-TMC2 micelles. Blank CA-TMC2 micelles were treated with the largest concentrations in this experiment, as medium control. After treatment for 20 hours, 10 μL of MTT dye solution was added to each well, and then, the plate was incubated for 4 hours at 37°C. Up to 100 μL of DMSO was added to each well, and the absorbance at 492 nm was recorded using an enzyme immunoassay instrument. The cytotoxicity of OST and OST/CA-TMC2 micelles were expressed as the percentage reduction of cell viability. In accordance with the cell viabilities of the dose-response curve, the concentration of the test compound was estimated to yield 50% of cell growth inhibition (IC50 value). The selective index was calculated by dividing the IC50 of Hela and MCF-7 cells.

Cell apoptosis assay

Hela and MCF-7 cells (5×10^4 cells per well) were exposed to control, 80 $\mu g \cdot mL^{-1}$ of OST, 420 $\mu g \cdot mL^{-1}$ of CA-TMC2 micelles, and 420 $\mu g \cdot mL^{-1}$ of OST/CA-TMC2 micelles for 24 hours and harvested in PBS. The cells were fixed in ice-cold 70% EtOH overnight, separated by centrifugation, treated with 1.0 $mg \cdot mL^{-1}$ RNase A (Beyotime Institute of Biotechnology, Haimen, People's Republic of China), and stained with 50 $\mu g \cdot mL^{-1}$ propidium iodide (PI). The stained cells were run through an FCM-FC500 (Beckman Coulter Inc, Brea, CA, USA). The results were presented as the number of cells versus the amount of DNA, as indicated by the intensity of fluorescence.

Hela and MCF-7 cells (5×10^4 cells per well) were exposed to OST, OST/CA-TMC, and CA-TMC2 for 24 hours and harvested by pancreatin. The cells were washed by PBS, and 200 μL of binding buffer was used to resuspend the cells. The cells were treated with 10 μL of annexin V-fluorescein isothiocyanate (FITC) for 15 minutes, away from light, and fixed with 300 μL of binding buffer. PI (50 μL) was added 5 minutes before FCM-FC500 detection.

Uptake process of OST/CA-TMC micelles observed by confocal laser scanning microscopy (CLSM)

The uptake of fluorescent OST/FITC-CA-TMC2 micelles by Hela and MCF-7 cells was visualized by CLSM (TCS-SP2, Leica Microsystems, Wetzlar, Germany). FITC-CA-TMC2 was synthesized by stirring 10 mg of FITC and 300 mg of CA-TMC2 in phosphate buffer (pH 9.12) for 24 hours, in the dark. The product was dialyzed in demineralized water for 4 days, in the dark, and then freeze-dried. OST was loaded in FITC-CA-TMC2 micelles as a fluorescence marker. Hela and MCF-7 cells were cultured in six-well plates at a density

of 1×10^5 cells/well and allowed to attach onto the cover slips during incubation for 24 hours. The cells were treated with OST-loaded FITC-CA-TMC2 micelles (240 $\mu g \cdot mL^{-1}$, including 40 $\mu g \cdot mL^{-1}$ OST). After incubation for 1, 2, 4 and 6 hours at 37°C, the supernatant was carefully removed, and the cells were washed thrice with ice-cold PBS and fixed with 4% formaldehyde. After the nucleus was stained with Hoechst 33258 (Beyotime Institute of Biotechnology) (10 $\mu g \cdot mL^{-1}$), the slides were mounted and imaged with a TCS-SP2 CLSM system.

Statistics

Values are expressed as mean ± standard deviation (SD). Data were analyzed by one-way analysis of variance (ANOVA) with the post hoc Tukey test applied for paired comparisons (SPSS 16; SPSS Inc, New York, NY, USA). The criterion of statistical significance was taken as $^*P < 0.05$, $^{**}P < 0.01$, or $^{\#}P < 0.05$, $^{\#\#}P < 0.01$.

Results and discussion

Synthesis of CA-TMC

The synthesis routes of the intermediate product, TMC, and novel polymer, CA-TMC, are shown in Figure 1. Different DQs of TMC were synthesized with CH_3I and chitosan by controlling the steps and the reaction time. Different TMCs were dissolved in deionized water and reacted with the active capric acids in methanol at 70°C for 24 hours. The TMC was then dissolved in methanol. This heterotrophic reaction resulted in novel polymer production. The CA-TMC was purified using 20% to 30% EtOH.

Characterization of CA-TMC

FTIR spectrum

In Figure 2B, the FTIR spectrum of TMC was different from that of chitosan (Figure 2A). A new deformation vibration peak of N-CH_3 appeared at 1,473 cm^{-1}, indicating that the hydrogen of the NH_2 in chitosan was replaced partly. This confirmed the formation of TMC. Comparing Figure 2C and B, CA-TMC2 was shown to have retained the characteristics of TMC2 and exhibited new signals. The CONH stretching bands were at 1,650 and 1,700 cm^{-1}, which corresponded to the amide group. The band intensity at 2,920 and 2,850 cm^{-1} corresponded to the stretching vibrations of $-CH_3$ and $-CH_2-$. The band at 620 cm^{-1} was the correlation absorption band of $-CO(CH_2)_8CH_3$. These signals confirmed the formation of CA-TMC.

^{1}H-NMR spectrum

The successful incorporation of chitosan, TMC2, and CA-TMC2 were further confirmed by the ^{1}H-NMR assay. Figure 3 shows the spectra of chitosan were: 3.59 (1-H), 2.32–2.89 (2H-6H), and 1.92 (NH_2); of TMC2 were: 5.2–5.7 (1-H), 3.79–4.05 (3H-6H), 4.22 (2-H), 3.0 [$-N + (CH_3)_3$], 3.4 [$-N(CH_3)_2$];[36] and of CA-TMC2 were: 5.2 (1-H), 2.91 (2-H), 3.4–4.4 (3-H–6-H), 3.3 [$-N + (CH_3)_3$], 2.5 [$-N(CH_3)_2$], 1.2 (R-H2-8), 0.8 (R-H9). In

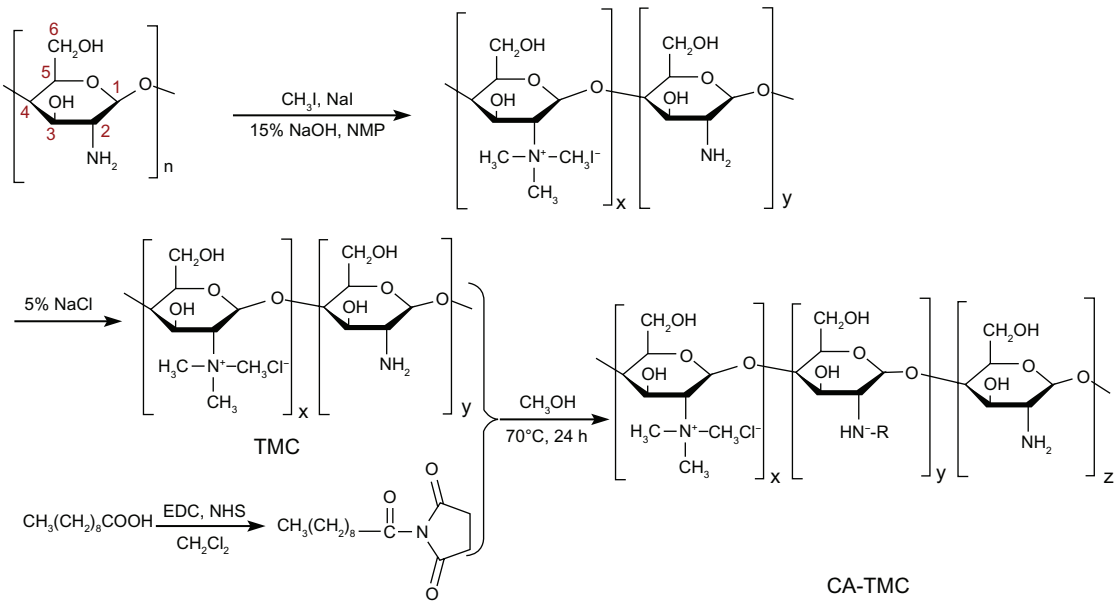

Figure 1 Synthesis route of TMC and CA-TMC.
Abbreviations: CA-TMC2, N-caprinoyl-N-trimethyl chitosan; TMC, N-trimethyl chitosan.

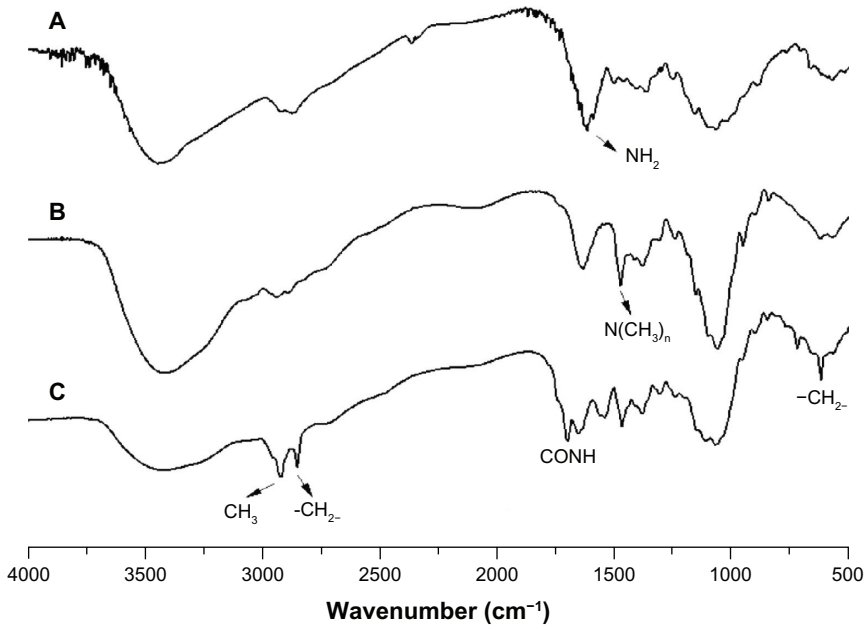

Figure 2 FTIR spectra of chitosan (**A**), TMC2 (**B**), and CA-TMC2 (**C**).
Abbreviations: CA-TMC2, N-caprinoyl-N-trimethyl chitosan; FTIR; Fourier transform infrared; TMC, N-trimethyl chitosan.

Figure 3C, the ^{1}H-NMR spectrum of CA-TMC2 was different from that of chitosan (Figure 3A) and TMC2 (Figure 3B). The peak of $-N^{+}(CH_3)_3$ and $-N(CH_3)_2$ appeared at δ 3.3 and δ 2.5. The signals of CH_2 and CH_3 of CA-TMC in the CA chain were corresponding to δ1.0 and δ 0.8, respectively, but the CH_2 and CH_3 signals of CA-TMC were weak in the D_2O solvent. We postulated the reason for this phenomenon might be that hydrophobic caprinoyl gathered in the micellar core due to self-aggregation so, DMSO-d6 was used as the solvent to destroy the self-aggregation structure. In Figure 4, a strong CH_2 signal appeared in CA-TMC. ^{1}H-NMR results further confirmed the formation of CA-TMC and also showed that CA-TMC possibly self-aggregated in D_2O.

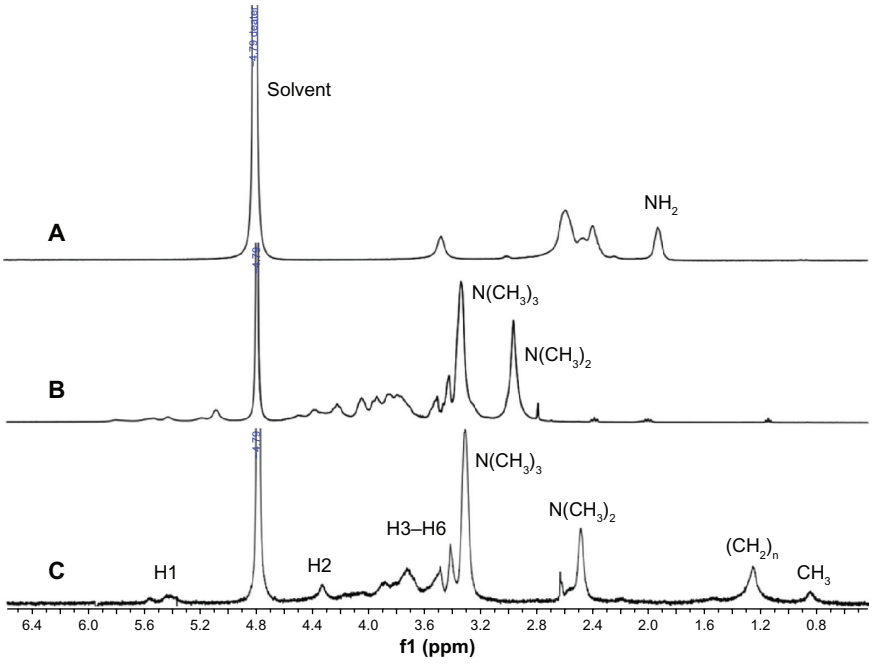

Figure 3 ^{1}H-NMR spectra of chitosan (**A**), TMC2 (**B**), and CA-TMC2 (**C**) in D_2O.
Abbreviations: CA-TMC, N-caprinoyl-N-trimethyl chitosan; ^{1}H-NMR, proton nuclear magnetic resonance; TMC, N-trimethyl chitosan.

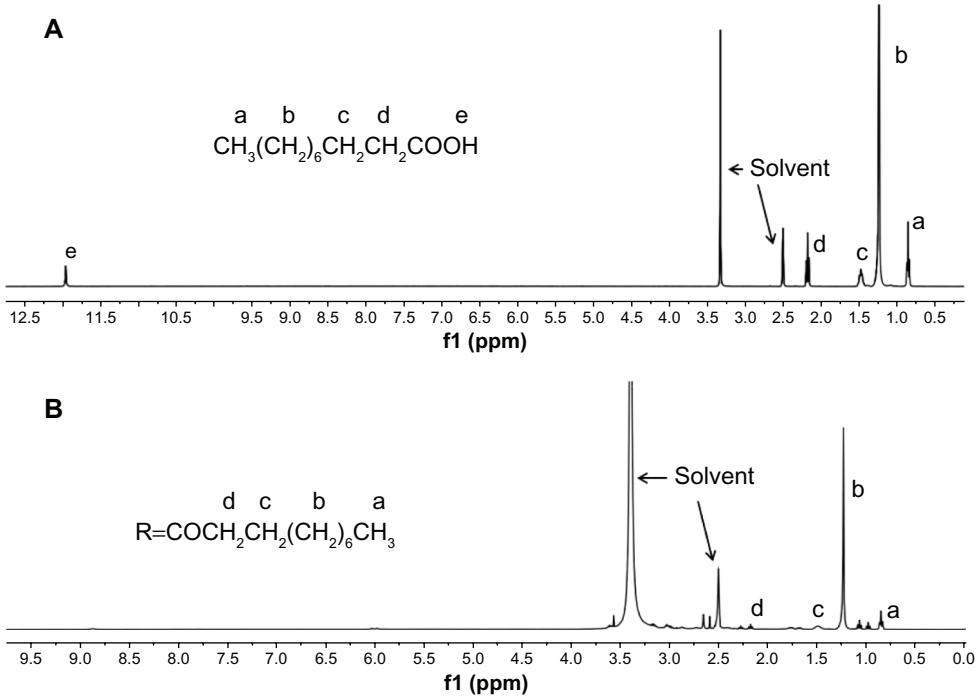

Figure 4 ^{1}H-NMR spectra of capric acid (**A**) and CA-TMC2 (**B**) in DMSO-d6.
Abbreviations: CA-TMC, N-caprinoyl-N-trimethyl chitosan; DMSO, dimethyl sulfoxide; ^{1}H-NMR, proton nuclear magnetic resonance.

Elemental analysis

The DQ and the DS of the trimethyl and CA groups were important parameters for CA-TMC. These were calculated, based on the elemental analysis data, by comparing the C and N molar ratios obtained using the previously described equations 1 and 2. All results are shown in Table 1. The standard deviation of the prepared polymers was between 1.6% and 4.2%. CA-TMC1, CA-TMC2, and CA-TMC3 indicate CA-TMC with DQ of the trimethyl groups 27.0%, 43.1%, and 62.0%, respectively. The DS of the CA group in CA-TMC1, CA-TMC2, and CA-TMC3 was 44.9%, 27.0%, 13.3%, respectively. The DS of CA-TMC decreased with the increase of DQ.

Table 1 Chemical compositions and properties of polymer micelles (n = 3)

Sample	N(C)/N(N)	Standard deviation (%)	Degree of quaternization (%)	Degree of substitution (%)
CS	5.5	0.2	–	–
TMC1	6.3	4.2	27.0	–
TMC2	6.8	2.2	43.1	–
TMC3	7.9	3.8	62.0	–
CA-TMC1	10.8	3.8	–	44.9
CA-TMC2	9.5	2.7	–	27.0
CA-TMC3	9.2	1.6	–	13.3

Notes: N(C)/N(N),the rate of the number of elemental carbon to the number of elemental nitrogen in polymer.
Abbreviations: CA-TMC, N-caprinoyl-N-trimethyl chitosan; CS, chitosan; TMC, N-trimethyl chitosan.

Self-assembly of CA-TMC

Micelles can be formed only when the polymer concentration is higher than its CMC, which has an important function in maintaining the micellar system stability. Figure 5 shows a typical plot of I_{372}/I_{383} versus logC of CA-TMC. A substantial increase of the intensity ratio was observed when the concentration was higher than the CMC, indicating nanomicelle formation. Therefore, the CMC was estimated as the intersection of two straight lines, of which one was the fitted line at low nanoaggregate concentrations and the other was the fitted line on the rapidly increasing part of the curve.

The CMC of CA-TMC1, CA-TMC2, and CA-TMC3 were 0.6, 21, and 88 $mg \cdot L^{-1}$, respectively. These values were significantly lower than those of low-molecular weight surfactant sodium dodecyl sulfate in water (2.3×10^3 $mg \cdot L^{-1}$) and deoxycholic acid-modified glycol chitosan that had a CMC of 47 $mg \cdot L^{-1}$ to 219 $mg \cdot L^{-1}$.[37,38] The low CMC of CA-TMC was attributed to the higher DS of CA chains with stronger hydrophobicity. The CMC of the polymer decreased with increase in DQ or decrease in DS. The low CMC suggests that CA-TMC micelles remain stable in solution, even after extreme dilution, and can preserve their stability, without dissociation, after IV injection into systemic circulation.

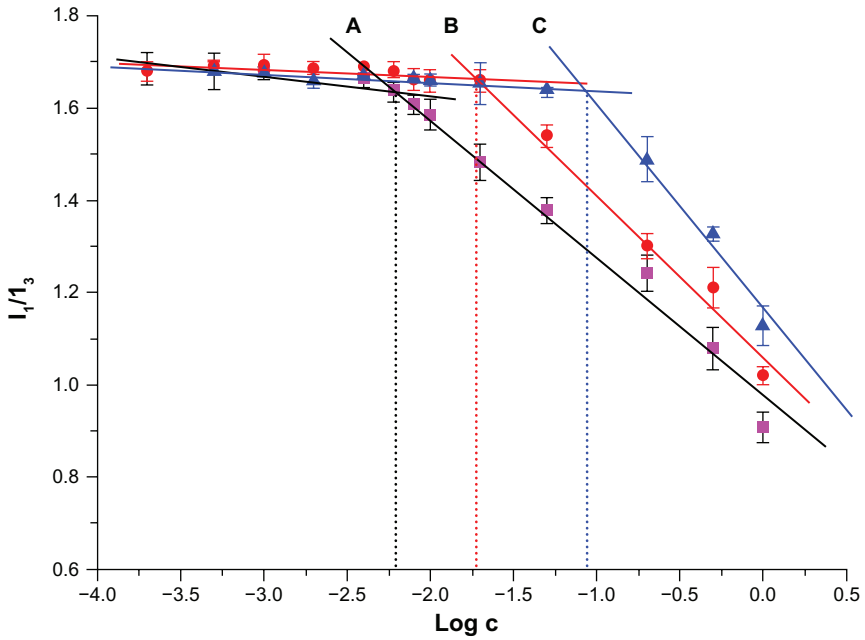

Figure 5 Coordinates of CA-TMC1 (**A**), CA-TMC2 (**B**), and CA-TMC3 (**C**) micellar solution at different concentrations.
Abbreviation: CA-TMC, N-caprinoyl-N-trimethyl chitosan.

Biocompatibility evaluation

Cytocompatibility

Cell cytotoxicity assays are among the most common in vitro bioassay methods used to predict the toxicity of substances in various tissues.[39,40] In this study, two tumor cell lines and a human normal liver cell line were used to evaluate the cytotoxicity of CA-TMC by MTT assay. The results show that CA-TMC micelles were practically nontoxic to Hela, MCF-7, and HL7702 (with cell viabilities of 84.4% to 101.7%) at concentrations of 0.5, 1.0, and 2.0 mg · mL^{-1}. CA-TMC micelles possess excellent biocompatibility, as shown in Figure 6. TMC is among the few synthetic water-soluble polymers approved for use in drug carriers, whereas CA is a natural antioxidant fatty acid.

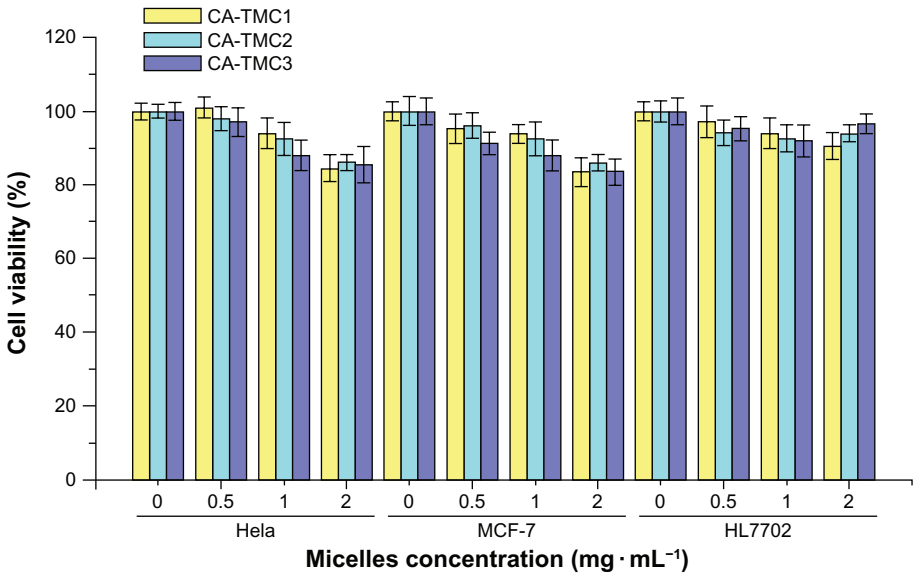

Figure 6 Cytocompatibility of CA-TMC1 CA-TMC2 and CA-TMC3 at different concentrations on Hela, MCF-7, and HL7702 cells.
Notes: The cells were identified using micelles for 48 hours. Data are presented as mean ± SD (n = 5).
Abbreviations: CA-TMC, N-caprinoyl-N-trimethyl chitosan; SD, standard deviation.

Therefore, CA-TMC copolymers are solely made of biocompatible components.

Hemolysis

Previous study suggested that the blood compatibility of chitosan and its derivates could be evaluated in terms of hemolysis.[41] Notara et al[42] investigated the hemocompatibility of chitosan-alginate physical gel, and the result showed that chitosan-alginate physical gel has excellent hemocompatibility and is suitable for further drug delivery application. Herein, the hemocompatibility of CA-TMC micelles and positive controls of Tween 80 and F188 were evaluated, and the results presented in Figure 7. The hemolysis rate of CA-TMC increased with the increasing DQs, but no significant difference was found ($P > 0.05$). At the concentration of 2.0 mg·mL^{-1}, the sample of CA-TMC showed about a 5% hemolysis ratio, which was far smaller than the 49.7% hemolysis ratio of Tween 80; the hemolysis of CA-TMC was similar to the hemolysis of F188. These results indicated that CA-TMC had excellent hemocompatibility and was suitable for various drug delivery applications.

Acute toxicity

To investigate the acute toxicity of CA-TMC, CA-TMC2 was chosen as the sample because of its nonsignificant difference in cell toxicity and hemolysis evaluation. Mice were injected with various doses of CA-TMC2 or physiological saline, through the tail vein. LD50 was used as a measurement. Toxic responses, such as prostration, piloerection, and respiratory distress, were observed at 12 hours after injection, and decreased appetite, and loose and watery stool were observed for the next 2 days in the surviving mice compared with the physiological saline group. After feeding for 14 days, the weight of the surviving mice of CA-TMC2 group and physiological saline group had no significant disparity. The LD50 of CA-TMC2 administered by IV injection was 368.79 mg·kg^{-1}, with 95% confidence limits of 333 mg·kg^{-1} to 407.25 mg·kg^{-1}.

To investigate the histopathological effect of CA-TMC2 on various organs, such as heart, liver, spleen, lung, and kidney, mice were administered CA-TMC2 IV at a half-dose of LD50. The histopathological changes in each organ were observed under light microscopy on day 8 after CA-TMC2 treatment (Figure 8). No histopathological changes were observed in the CA-TMC2-treated groups compared with the physiological saline group, which indicates that CA-TMC2 micelles had no significant toxicity on the main organs.

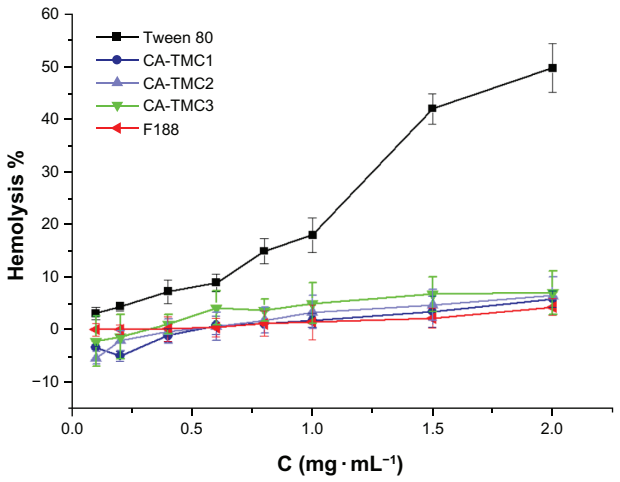

Figure 7 Hemolysis evaluation of Tween 80, CA-TMC1, CA-TMC2, CA-TMC3, and F188 using erythrocytes freshly harvested from rabbit blood.
Abbreviation: CA-TMC, N-caprinoyl-N-trimethyl chitosan.

Preparation and characteristics of OST-loaded CA-TMC micelles

The main characteristics of the blank micelles and OST-loaded micelles are shown in Table 2. The sizes of all the micelles slightly increased after OST loading. The zeta potentials of the blank micelles with different DQs were highly positive charges. The zeta potentials slightly decreased with increase in DQ but remained above 32 mV after OST loading. The highly positive zeta potentials suggested that the CA-TMC micelles promoted the internalization rate, further increased cellular uptake and escape from lysosomes after internalized, and increased perinuclear localization; the nanoparticles with negatively and neutrally charged can highly colocalize with lysosomes.[43] The EE and the DL of OST-loaded micelles initially increased and then decreased. The OST/CA-TMC2 micelles showed the highest EE (79.1%) and DL (19.1%). At a loading level of 19.1%, 1 mg·mL^{-1} OST/CA-TMC micelles contained 191 μg·mL^{-1} OST, which was 81 times higher than its intrinsic water solubility of 2.36 μg·mL^{-1}.

When the stability of these micelles was observed at room temperature, OST crystals were found to have seeded out from the OST/CA-TMC3 micelles in 6 hours. Some floccules were observed in the OST/CA-TMC1 micelle solution at 24 hours. After 48 hours, the crystals and precipitation was OST/CA-TMC2 < OST/CA-TMC < OST/CA-TMC3.

The morphology of the OST/CA-TMC2 micelle is shown in Figure 9. The scanning electron microscope (SEM) and AFM images displayed a spherical morphology. The average diameter was 170 nm, which was smaller than the size

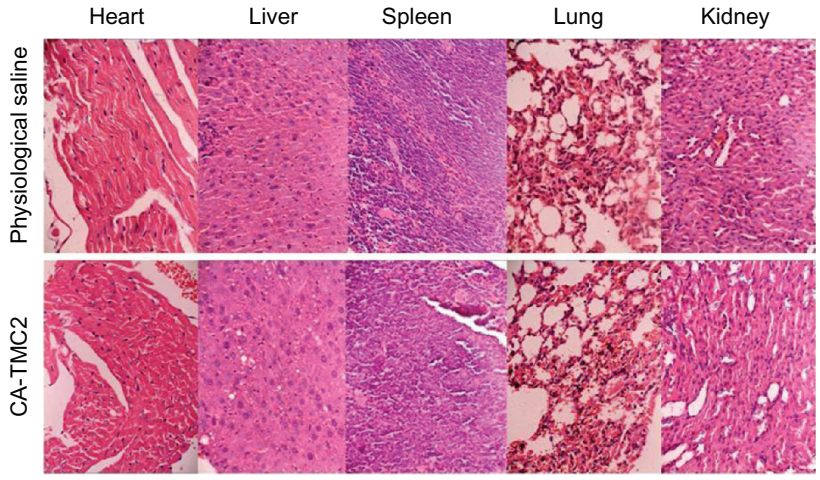

Figure 8 Tissue slice of the physiological saline group and the CA-TMC2 group (×100).
Abbreviation: CA-TMC2, N-caprinoyl-N-trimethyl chitosan.

detected by DLS because of the collapse of the outer shell during the drying process.

In vitro release of OST from OST/CA-TMC2 micelles

The in vitro release profiles of the OST and OST/CA-TMC2 micelles were evaluated at 37°C in phosphate buffer (10% EtOH) at pH 7.4 and 5.0, respectively. The results are shown in Figure 10. The release rate of OST was fast, with 80% released in only 2 hours, indicating that the bag filters did not hinder drug release. The OST/CA-TMC2 micelles showed a slower release than OST, with 70% released in 24 hours, indicating that the OST/CA-TMC2 micelles delayed the release. The sustained release rate can be accelerated at pH 5.0, possibly a profit for antitumor treatment because of the lower pH of tumor cells than normal cells.

In vitro antitumor activity of OST-loaded micelles

MTT assay

To investigate the in vitro antitumor activity of the OST/CA-TMC micelles, two established OST-susceptible human tumor cell lines were treated with different drug concentrations for 24 hours.[45,46] MTT colorimetric assay was then performed to evaluate the cytotoxic effect of OST/CA-TMC micelles and the positive control drug, OST. The results are shown in Figure 11. The antitumor activities of OST and OST/CA-TMC micelles were studied in Hela and MCF-7 cells.

OST/CA-TMC2 micelles clearly inhibited the growth of Hela and MCF-7 cells in vitro in a dose-dependent manner. Statistically significant differences in cell viability were observed among the cells treated with different preparations. The IC50 of OST-administered Hela and MCF-7 cells were approximately 51.0 and 83.2 $\mu g \cdot mL^{-1}$, respectively. The IC50 of Hela and MCF-7 cells were 35.8 and 46.7 $\mu g \cdot mL^{-1}$ for OST/CA-TMC2 micelles, respectively. The results show that the OST/CA-TMC22 micelles enhanced the antitumor effect of OST. When the OST concentration was below 40 $\mu g \cdot mL^{-1}$, OST/CA-TMC2 micelles had higher cell vitality. For in vivo applications, OST would need more time to be released from the micelles, and the tumor cells were not likely treated with free OST at such a high concentration for a long time. The antitumor activity of OST/CA-TMC micelles can be enhanced by placing targeting ligands,

Table 2 Characteristics of OST/CA-TMC micelles

Sample	CA-TMC micelles		OST/CA-TMC micelles				
	Zeta potential (mV)	Size (nm)	Zeta potential (mV)	Size (nm)	Polydispersity index	EE (%)	DL (%)
CA-TMC1	35.1	212.7 ± 26.1	32.9	285.5 ± 32.9	0.3	73.2	17.8
CA-TMC2	48.6	168.3 ± 19.0	43.7	192.0 ± 25.4	0.2	79.1	19.1
CA-TMC3	56.8	136.5 ± 15.4	52.4	184.7 ± 20.9	0.2	64.3	16.1

Abbreviations: CA-TMC, N-caprinoyl-N-trimethyl chitosan; DL, drug loading; EE, encapsulation efficiency; OST/CA-TMC, osthole-loaded N-caprinoyl-N-trimethyl chitosan.

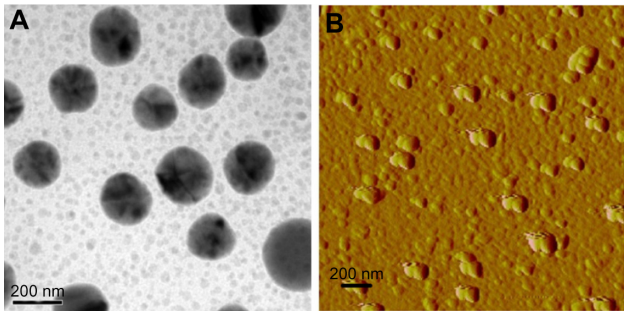

Figure 9 TEM image (**A**) of OST/CA-TMC2 micelles; AFM images (**B**) of OST/CA-TMC2 micelles.
Abbreviations: AFM, atomic force microscopy; OST/CA-TMC2, osthole-loaded N-caprinoyl-N-trimethyl chitosan; TEM, transmission electron microscope.

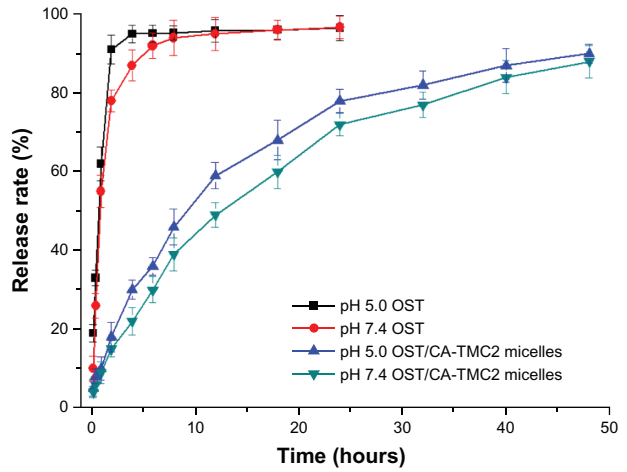

Figure 10 In vitro release of OST in pH 5.0 PBS and pH 7.4 PBS; OST/CA-TMC2 micelles in pH 5.0 PBS and pH 7.4 PBS.
Abbreviations: OST, osthole; OST/CA-TMC2, osthole-loaded N-caprinoyl-N-trimethyl chitosan; PBS, phosphate-buffered saline.

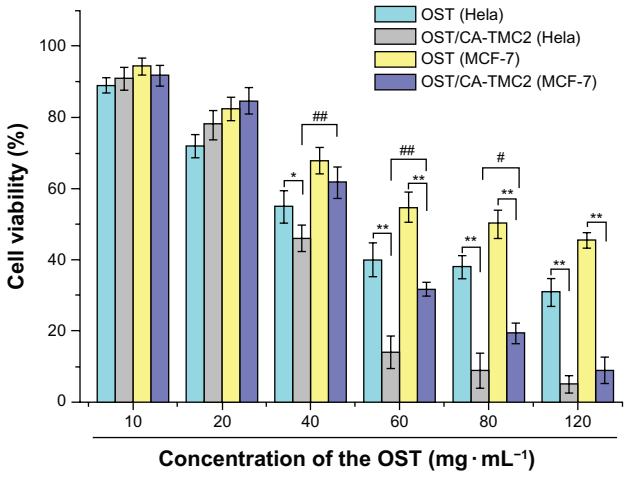

Figure 11 Cytotoxic effects of OST against Hela and MCF-7 and OST/CA-TMC2 against Hela and MCF-7, respectively (n = 5).
Notes: $^{*}P < 0.05$ vs OST group; $^{**}P < 0.01$ vs OST group; or $^{\#}P < 0.05$ vs OST/CA-TMC group; $^{\#\#}P < 0.01$ vs OST/CA-TMC group.
Abbreviations: OST, osthole; OST/CA-TMC2, osthole-loaded N-caprinoyl-N-trimethyl chitosan.

such as folic acid and antibody fragments, on the micelle surface, to facilitate specific cellular uptake of micelles.[45] These micelles have several uniquely integrated indispensable features, such as excellent biocompatibility, superior stability, high DL, increased cellular uptake, and perinuclear localization, which provide an advanced platform for tumor-targeting drug delivery.

Cell apoptosis assay

DNA fragmentation and hypodiploid cells emerge at late-stage apoptosis.[47] To detect early apoptosis and to distinguish apoptosis from necrosis, cells were treated with annexin V-FITC and PI. At this point in time, no reports exist that describe the mechanism through which OST kills Hela and MCF-7 cells. The current study is the first to discover that OST induces Hela and MCF-7 cell death via the apoptosis pathway. These results are shown in Figure 12 and Table 3. No visible apoptosis and necrosis were observed in the control cells (Figure 12A). Only a small amount of necrotic (or late-apoptotic) cells and early-apoptotic cells were found in the cells treated with CA-TMC2 micelles (Figure 12B). Necrotic (or late-apoptotic) cells and early-apoptotic cells were observed in OST-treated cells (Figure 12C) and OST/CA-TMC2 micelles (Figure 12D). OST/CA-TMC2 micelles significantly enhanced the total number of apoptotic cells compared with OST. Most of the apoptotic cells were early-apoptotic cells (Table 3). Therefore, the inhibitory effect of OST on cell viability resulted from its apoptosis-inducing activity.

Cell internalization observed by CLSM

The cellular uptake and intracellular release behaviors of OST/CA-TMC micelles were investigated by CLSM. OST/CA-TMC2 micelles were incubated with Hela and MCF-7 cells at 37°C for 1, 2, 4, and 6 hours, respectively. As shown in Figure 13, after 1 hour of incubation, the OST/CA-TMC2 micelles were observed only in the cytoplasm and the green fluorescence was weak. When the cells were exposed to OST/CA-TMC2 micelles for 2 hours, more intense fluorescence was observed in the cytoplasm. At 4 hours, the green fluorescence was surrounding the nuclei and partially merged with the nuclei of Hela and MCF-7 cell. At 6 hours, the cells incubated with OST/CA-TMC2 micelles emitted significantly increased fluorescence in the cell nuclei, and no green fluorescence was observed in the cytoplasm. These data demonstrate that these positively charged CA-TMC micelles are efficient vehicles that can be used to transport OST into the

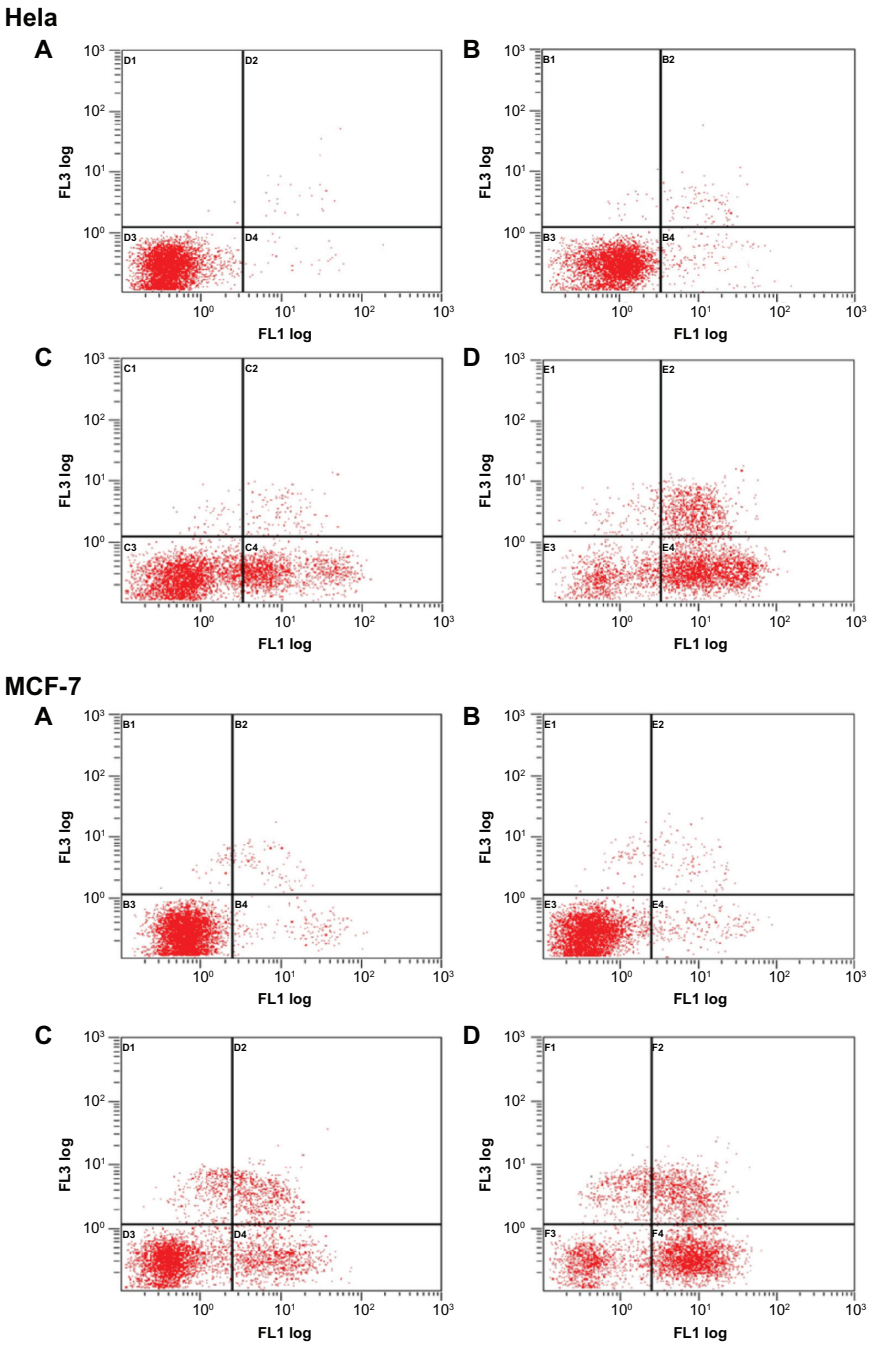

Figure 12 Apoptosis evaluation after Hela and MCF-7 cells were treated with negative control (**A**), 420 μg·mL^{-1} of CA-TMC2 micelles (**B**), 80 μg·mL^{-1} of OST (**C**), and 420 μg·mL^{-1} of OST/CA-TMC2 micelles including 80 μg·mL^{-1} of OST (**D**).
Abbreviations: OST, osthole; OST/CA-TMC2, osthole-loaded N-caprinoyl-N-trimethyl chitosan.

Table 3 Cell apoptosis of Hela and MCF-7 cells

Group	Cell population of Hela				Cell population of MCF-7			
	%*	%**	%§	%†	%*	%**	%§	%†
Control	0.1	0.5	98.8	0.6	0.3	2.5	93.2	4.0
CA-TMC2 micelles	0.1	1.8	94.6	3.5	0.4	3.9	90.2	5.5
OST	1.0	2.8	60.2	36.0	6.7	12.6	62.5	18.1
OST/CA-TMC2 micelles	1.7	22.7	17.1	58.5	9.0	20.6	23.1	47.3

Notes: *Unviable cell; **necrosis (or late apoptosis) cell; §viable cell; †early apoptosis cell.
Abbreviations: CA-TMC, N-caprinoyl-N-trimethyl chitosan; OST, osthole; OST/CA-TMC, osthole-loaded N-caprinoyl-N-trimethyl chitosan.

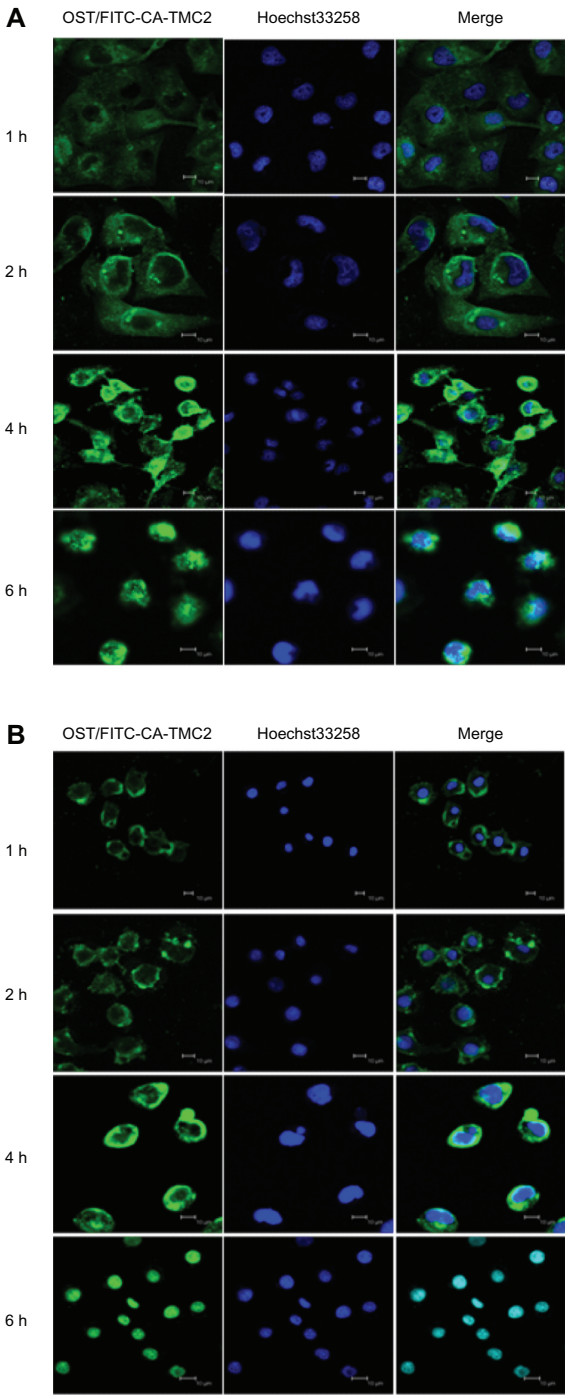

Figure 13 CLSM images showing the uptake and subcellular localization of Hela (**A**) and MCF-7 (**B**).
Abbreviations: CLSM, confocal laser scanning microscope; OST/TITC-CA-TMC2, osthole loaded in N-caprinoyl-N-trimethyl chitosan with fluoredcein isothiocyanate marking.

cytoplasm, that they can escape from lysosomes after being internalized, and that they exhibit perinuclear localization. The cytotoxicity results demonstrate that the growth of Hela and MCF-7 cells can be effectively inhibited by OST/CA-TMC2 micelles.

Conclusion

In this study, novel nanomicelles based on chitosan and various amounts of trimethyl and CA chains were synthesized and characterized. CA-TMC exhibited a low CMC, above which the amphiphilic derivatives self-assembled in an aqueous environment to form micelles. The biocompatibility and nontoxicity of CA-TMC as excipients for the formulations aimed at IV administration were confirmed in this study. Furthermore, OST, a water-insoluble antitumor drug, was successfully loaded into the CA-TMC micelles using a simple ultrasound method. The DL capacity of OST was significantly affected by the DQ of the trimethyl and the DS of CA chains. The EE, DL, and zeta-potential were superior features of the OST-loaded micellar system and were 79.1%, 19.1%, and 43.7 mV, respectively. The OST-loaded micelles delayed the release of OST. The sustained release rate was accelerated under the conditions of pH 5.0. The in vitro cytotoxicity assay also showed that blank micelles had limited inhibitory activity, without significant dose dependence. The cytotoxicity of each kind of drug-carrying micelle was greater than the sum of the cytotoxicities of OST and their corresponding blank micelles; this result suggests that the cytotoxicity of each formulation displayed a synergistic effect, rather than a simple additive effect, between drug and carrier. The apoptosis assays indicated that the cytotoxicity of OST on Hela and MCF-7 cells was induced by apoptosis. Incorporating OST into micelles did not change the apoptosis pathway and enhanced the apoptosis effect. The CLSM images exhibited that OST/CA-TMC micelles could localize in the nuclei. The results of this research demonstrate the potential of CA-TMC2 as an alternative and promising carrier for micelles of OST and other similar hydrophobic anticancer agents.

Acknowledgements

This work was supported by the National Natural Science Foundation Projects of the People's Republic of China (No 81273463), the Jiangsu Science and Technology Support Plan (BE2011670), the National Student and Innovative Experimental Plan (111028533, Microcomputer No 5731503311), and the Priority Academic Program Development of Jiangsu Higher Education Institutions (PAPD).

Disclosure

The authors report no conflicts of interest in this work.

References

1. Liang HJ, Suk FM, Wang CK, Hung LF, Chen NQ, Chen YC, Chang CC, Liang YC . Osthole, a potential antidiabetic agent, alleviates hyperglycemia in db/db mice. *Chem Biol Interact*. 2009;181(3):309–315.
2. Ming LG, Zhou J, Cheng GZ, Ma HP, Chen KM. Osthol, a coumarin isolated from common cnidium fruit, enhances the differentiation and maturation of osteoblasts in vitro. *Pharmacology*. 2011;88(1–2):33–43.
3. Nakamura T, Kodama N, Arai Y, Kumamoto T, Hiquchi Y, Chaichantipyuth C, Ishikawa T, Ueno K, Yano S. Inhibitory effect of oxycoumarins isolated from the Thai medicinal plant Clausena guillauminii on the inflammation mediators, iNOS, TNF-alpha, and COX-2 expression in mouse macrophage RAW 264.7. *J Nat Med*. 2009;63(1):21–27.
4. He Y, Qu S, Wang J,He X, Lin W, Zhen H, Zhang X. Neuroprotective effects of osthole pretreatment against traumatic brain injury in rats. *Brain Res*. 2012;1433:127–136.
5. Hsieh MT, Hsieh CL, Wang WH, Chen CS, Lin CJ, Wu CR. Osthole improves aspects of spatial performance in ovariectomized rats. *Am J Chin Med*. 2004;32(1):11–20.
6. Okamoto T, Kobayashi T, Yoshida S. Chemical aspects of coumarin compounds for the prevention of hepatocellular carcinomas. *Curr Med Chem Anticancer Agents*. 2005;5(1):47–51.
7. Yang D, Gu T, Wang T, Tang Q, Ma C. Effects of osthole on migration and invasion in breast cancer cells. *Biosci Biotechnol Biochem*. 2010;74(7):1430–1434.
8. Xu X, Zhang Y, Qu D, Jiang T, Li S. Osthole induces G2/M arrest and apoptosis in lung cancer A549 cells by modulating PI3K/Akt pathway. *J Exp Clin Cancer Res*. 2011;30:33.
9. Kao SJ, Su JL, Chen CK, Yu MC, Bai KJ, Chang JH, Bien MY, Yang SF, Chien MHl. Osthole inhibits the invasive ability of human lung adenocarcinoma cells via suppression of NF-κB-mediated matrix metalloproteinase-9 expression. *Toxicol Appl Pharmacol*. 2012;261(1):105–115.
10. Guo BF, Liu S, Ye YY, Han XH. Effects of the components of osthole, psoralen, paeonol on breast cancer MDA-MB-231BO cell lines inhibition and TGF-βl gene expression in vitro. *China Journal of Traditional Chinese Medicine and Pharmacy*. 2012;27(2):430–433.
11. Zhang XD, Yu YM, Fan CL, Liu W. Osthol adriamycin cardiac toxicity and mechanism of the protective effect of study. *Acta Chinese Medicine and Pharmacology*. 2010;38(4):34–37.
12. Hu XB, Liu Y, Bei YY, Zhao J, Zhang XN. Preparation of pH-sensitive osthol-nanoparticles and its pharmacokinetics in rats. *Chinese Journal of New Drugs*. 2012;21(5):490–456.
13. Dash M, Chiellini F, Ottenbrite RM, Chiellini E. Chitosan-A versatile semi-synthetic polymer in biomedical applications. *Prog Polym Sci*. 2011;36(8):981–1014.
14. Jayakumar R, Prabaharan M, Nair SV, Tamura H. Novel chitin and chitosan nanofibers in biomedical applications. *Biotechnol Adv*. 2010;28(1):142–150.
15. Kong M, Chen XG, Xing K, Park HJ. Antimicrobial properties of chitosan and mode of action: a state of the art review. *Int J Food Microbiol*. 2010;144(1):51–63.
16. Muzzarelli RAA, Tanfani F. The N-permethylation of chitosan and the preparation of N-trimethyl chitosan iodide. *Carbohydr Polym*. 1985;5(4):297–307.
17. Domard A, Rinaudo M, Terrassin C. New method for the quaternization of chitosan. *Int J Biol Macromol*. 1986;8(2):105–107.
18. Hamman JH, Schultz CM, Kotzé AF. N-trimethyl chitosan chloride: optimum degree of quaternization for drug absorption enhancement across epithelial cells. *Drug Dev Ind Pharm*. 2003;29(2):161–172.
19. Chen F, Zhang ZR, Yuan F, Qin X, Wang M, Huang Y. In vitro and in vivo study of N-trimethyl chitosan nanoparticles for oral protein delivery. *Int J Pharm*. 2008;349(1–2):226–233.
20. Chen H, Wu J, Sun M, Guo C, Yu A, Cao F, Zhao L, Tan Q, Zhai G. N-trimethyl chitosan chloride-coated liposomes for the oral delivery of curcumin. *J Liposome Res*. 2012;22(2):100–109.
21. Di Colo G, Burgalassi S, Zambito Y, Monti D, Chetoni P. Effects of different N-trimethyl chitosans on in vitro/in vivo ofloxacin transcorneal permeation. *J Pharm Sci*. 2004;93(11):2851–2862.
22. Amidi M, Romeijn SG, Borchard G, Junginger HE, Hennink WE, Jiskoot W. Preparation and characterization of protein-loaded N-trimethyl chitosan nanoparticles as nasal delivery system. *J Control Release*. 2006;111(1–2):107–116.
23. Li HY, Birchall J. Chitosan-modified dry powder formulations for pulmonary gene delivery. *Pharm Res*. 2006;23(5):941–950.
24. du Plessis LH, Kotzé AF, Junginger HE. Nasal and rectal delivery of insulin with chitosan and N-trimethyl chitosan chloride. *Drug Deliv*. 2010;17(6):399–407.
25. Croy SR, Kwon GS. Polymeric micelles for drug delivery. *Curr Pharm Des*. 2006;12(36):4669–4684.
26. Tian Y, Mao S. Amphiphilic polymeric micelles as the nanocarrier for peroral delivery of poorly soluble anticancer drugs. *Expert Opin Drug Deliv*. 2012;9(6):687–700.
27. Ye YQ, Chen FY, Wu QA, Hu FQ, Du YZ, Yuan H, Yu HY. Enhanced cytotoxicity of core modified chitosan based polymeric micelles for doxorubicin delivery. *J Pharm Sci*. 2009;98(2):704–712.
28. Gupta M, Agrawal GP, Vyas SP. Polymeric nanomedicines as a promising vehicle for solid tumor therapy and targeting. *Curr Mol Med*. 2013;13(1):179–204.
29. Mahmud A, Xiong XB, Aliabadi HM, Lavasanifar A. Polymeric micelles for drug targeting. *J Drug Target*. 2007;15(9):553–584.
30. Gong J, Chen M, Zheng Y, Wang S, Wang Y. Polymeric micelles drug delivery system in oncology. *J Control Release*. 2012;159(3): 312–323.
31. Niu C, Sun Q, Zhou J, Cheng D, Hong G. Folate-functionalized polymeric micelles based on biodegradable PEG-PDLLA as a hepatic carcinoma-targeting delivery system. *Asian Pac J Cancer Prev*. 2011;12(8):1995–1999.
32. Snyman D, Hamman JH, Kotze JS, Rollings JE, Kotzé AF. The relationship between the absolute molecular weight and the degree of quaternisation of *N*-trimethyl chitosan chloride. *Carbohydr Polym*. 2002;50(2):145–150.
33. Senso A, Franco P, Oliveros L, Minguillón CA. Characterization of doubly substituted polysaccharide derivatives. *Carbohydr Res*. 2000;329(2):367–376.
34. Yang YQ, Zheng LS, Guo XD, Qian Y, Zhang LJ. pH-Sensitive micelles self-assembled from amphiphilic copolymer brush for delivery of poorly water-soluble drugs. *Biomacromolecules*. 2011;12(1):116–122.
35. Huo M, Zhang Y, Zhou J, Zou A, Yu D, Wu Y, Li J, Li H. Synthesis and characterization of low-toxic amphiphilic chitosan derivatives and their application as micelle carrier for antitumor drug. *Int J Pharm*. 2010;394(1–2):162–173.
36. Sieval AB, Thanou M, Kotze AF, Verhoef JC, Brussee J, Junginger HE. Preparation and NMR characterization of highly substituted N-trimethyl chitosan chloride. *Carbohydr Polym*. 1998;36(2):157–165, 169.
37. Lee KY, Jo WH, Kwon IC, Kim YH, Jeong SY. Structural determination and interior polarity of self-aggregates prepared from deoxycholic acid-modified chitosan in water. *Macromolecules*.1998;31(2):378–383.
38. Kim SC, Yoon HJ, Lee JW, Yu J, Park ES, Chi SC. Investigation of the release behavior of DEHP from infusion sets by paclitaxel-loaded polymeric micelles. *Int J Pharm*. 2005;293(1–2):303–310.
39. Jia Y, Hu Y, Zhu Y, Che L, Shen Q, Zhang J, Li X. Oligoamines conjugated chitosan derivatives: synthesis, characterization, in vitro and in vivo biocompatibility evaluations. *Carbohydr Polym*. 2011;83(3):1153–1161.
40. Deng J, Gao N, Wang Y,Yi H, Fang S, Ma Y, Cai L. Self-assembled cationic micelles based on PEG-PLL-PLLeu hybrid polypeptides as highly effective gene vectors. *Biomacromolecules*. 2012;13(11):3795–3804.
41. Yang Y, Zhou Y, Chuo H, Wang S, Yu J. Blood compatibility and mechanical properties of oxidized-chitosan films. *J Appl Polym Sci*. 2007;106(1):372–377.
42. Notara M, Scotchford CA, Grant DM, Weston N, Roberts GA. Cytocompatibility and hemocompatibility of a novel chitosan-alginate gel system. *J Biomed Mater Res A*. 2009;89(4):854–864.
43. Yue ZG, Wei W, Lv PP, Yue H, Wang LY, Su ZG, Ma GH. Surface charge affects cellular uptake and intracellular trafficking of chitosan-based nanoparticles. *Biomacromolecules*. 2011;12(7):2440–2446.

44. Chou SY, Hsu CS, Wang KT, Wang MC, Wang CC. Antitumor effects of Osthol from Cnidium monnieri: an in vitro and in vivo study. *Phytother Res*. 2007;21(3):226–230.
45. Yang D, Wang H, Peng Y. Effects of osthole on the proliferation, cell cycle and apoptosis in human breast cancer cells. *Journal of Nanjing Normal University (Natural Science Edition)*. 2010;33(2):76–80.
46. Zhu H, Liu F, Guo J, Xue J, Qian Z, Gu Y. Folate-modified chitosan micelles with enhanced tumor targeting evaluated by near infrared imaging system. *Carbohydr Polym*. 2011;86(3):1118–1129.
47. Gorczyca W, Gong J, Darzynkiewicz Z. Detection of DNA strand breaks in individual apoptotic cells by the in situ terminal deoxynucleotidyl transferase and nick translation assays. *Cancer Res*. 1993;53(8):1945–1951.